Decomposition of benzene as a tar analogue in CO_2 and H_2 carrier gases, using a non-thermal plasma.

Faisal Saleem, Kui Zhang, Adam P. Harvey*

School of Engineering, Newcastle University Newcastle upon Tyne NE1 7RU

Abstract

Cracking of benzene in a non-thermal plasma (NTP) dielectric barrier discharge reactor (DBD) was investigated in CO_2 and H_2 carrier gases. Benzene was acting as an analogue for gasification tar, and CO_2 and H_2 are abundant in gasifier product gas. A parametric study in terms of specific input energy (SIE), residence time, concentration and temperature was performed to determine the optimal conditions for tar conversion. It was found that almost complete removal of benzene (36 g/Nm^3) was observed in each carrier gas at 30 kJ/L and at 4.23 s. Lower hydrocarbons ($<C_6$) (LHC) and solid residue were common products in both carrier gases. The selectivity to LHC in H_2 carrier gas was higher (12 %) than CO_2 (2 %) carrier gas, and CO was the major gaseous product in CO_2 carrier gas. However, the problem of solid formation in the reactor was completely eradicated by operating at elevated temperatures in H_2 carrier gas. The selectivity to lower hydrocarbons increased with increasing temperature. At 400^{o}C in H_2 carrier gas, the selectivity to LHC reached 91% with no formation of solid residue. The major lower hydrocarbons at these conditions were CH_4 (82 %) and C_2 (C_2H_6 +C_2H_4) 6.6 %.

Keywords: gasification, tar, non-thermal plasma, dielectric barrier discharge

1. Introduction

Compared to fossil fuel, the advantage of the biomass is the net neutral emission of CO_2 greenhouse gas. Hence, it is used as a source of renewable energy [1]. Its use is gaining attention due to global warming associated with fossil fuels [2]. Biomass gasification is a promising route to produce not only energy, but also CO and H_2 (syngas). The product gas can be used to produce hydrocarbons, CH_3OH, natural gas, hydrogen and various value-added chemicals. It has also direct applications in gas engines, turbines, furnaces, fuel cells and boilers [3]. However, the product gas from the gasifier is contaminated with particulate matter, tar and some other pollutants. In the practical application of biomass gasification, the formation of tar is the key issue which needs to be resolved due to its condensation on downstream filters, fuel line, and engine and turbine parts. Operational costs can be significantly increased by plugging, blocking and corrosion of the downstream equipment. Therefore, it is very important to remove problematic tar compounds for the successful application of producer gas [3-5].

There are various methods which can be used to decompose tar compounds at the downstream of the gasifier. These methods can be physical or chemical. In physical methods, tars are only captured by changing from one form to another, which produces additional waste streams, and generates secondary pollution. Furthermore, the associated chemical energy in the tars is also wasted [4]. Cyclone, dry/wet scrubber, electrostatic precipitator, rotating particle separators and tar filters can be used to remove tar by physical means.

For chemical treatment of tar, a process unit or secondary reactor is required to decompose the tar completely. The conversion of tar compounds into combustible components such as carbon monoxide and hydrogen can increase the calorific content of syngas [6]. These chemical methods are categorised as thermal cracking and catalytic cracking.

Thermal and catalytic cracking techniques have been employed to eliminate condensable tar compounds, but these methods also have drawbacks. The high temperatures and residence times required significantly increase the operational cost of thermal cracking [7]. For lower temperature operations, the use of catalysts is a better option to crack the tar contents into valuable gaseous products [8] [9]. Catalysts decompose the tar compounds by lowering the activation energy, and the cracking can take place at lower temperatures than in thermal cracking [10]. Metallic or non-metallic catalysts have been used to remove the tar compounds [11]. Nickel-based catalysts (metallic) have been extensively used to address the tar problem, and many researchers have reported high removal efficiency of tar compounds in the presence of nickel-based catalysts [11-13]. However, the use of catalysts has been inhibited by drawbacks including the process complexity, deactivation of catalysts due to sintering and/or carbon deposition, poisoning, fouling and regeneration [10]. Furthermore, thermal efficiency and composition of product gas also negatively affected by catalytic bed [14].

Hence, complete removal of tar remains a significant challenge due to its complex nature and the unavailability of proven, effective technology. In both thermal and catalytic cracking, the creation and stabilization of reactive species play key roles by initiating the necessary chemical reactions under thermodynamic and kinetic limitations. Similar processes (creation of reactive species) can be expected when using plasmas in which energetic electrons produce reactive species due to collision with molecules. However, the production of radicals of gas phase increases the removal efficiency of tar compounds [15]. The tar decomposition takes place due to the presence of an electro-radical atmosphere that initiates chemical reactions. Therefore the use of plasma reduces the requirement of severe operating conditions (high temperatures) as compared to thermal treatment. Hence, NTPs (Non-thermal plasmas) could be a promising and attractive route to produce the relatively clean product gas.

Various types of non-thermal plasmas have been investigated to decompose tar compounds. Jamroz *et al* (2018) investigated the steam reforming of tar representative compound in microwave plasma. Tar compounds were converted to CO, CO_2 and hydrogen in the presence of steam [16]. The performance of a gliding arc discharge reactor was studied by Zhu *et al* (2016). They reported 95 % conversion of the toluene, and the major products were acetylene and hydrogen [17]. In another study, the decomposition of toluene as a biomass tar representative was studied in gliding arc discharge reactor. It was reported that conversion and energy efficiency of toluene increased by adding the steam [18]. In many studies, the dielectric barrier discharge (DBD) reactor was used for cleaning gases [19-22]. It was observed that 74 % of the toluene is converted at specific input energy of 360 J/L [19]. However, the conversion decreased with increasing flow rate and concentration [23].

In this study, a DBD reactor was used to investigate the decomposition of benzene in CO_2 and H_2 carrier gases. Benzene was selected as a model compound due to its thermal stability and it has been reported as a tar representative in many experimental studies [24-30]. Moreover, the effect of each carrier gas on the product selectivity was also studied. CO_2 and H_2 are present in significant amounts (62-75%) in product gas [31]. Therefore, for a good understanding of tar removal in NTP to clean the product gas, it was very important to study the effect of both carrier gases individually. The effect of different parameters (SIE, residence time, concentration and temperature) was also investigated to study the performance of DBD reactor.

2. Materials and methods

2.1 Experimental setup

Fig. 1 shows a schematic of the experimental setup. The dielectric barrier discharge (DBD) consisted of two coaxial quartz tube (inner and outer tube). Outer tube has inner diameter of 15 mm, length 330 mm, while inner tube has the outer diameter of 12 mm, length 130 mm. The

one end of the inner tube is closed to allow the flow through annular space. Two metallic electrodes of stainless steel were used, one inside the inner tube and other outside external tube. The length of the discharge zone can be controlled by varying the size of external electrode (45 mm). The plasma was formed in the annular space of the coaxial cylindrical tubes. The plasma power provided to the reactor was controlled by using a variac which connected with plasma generator. The plasma generator provides the power to DBD reactor at a frequency of 20 kHz.

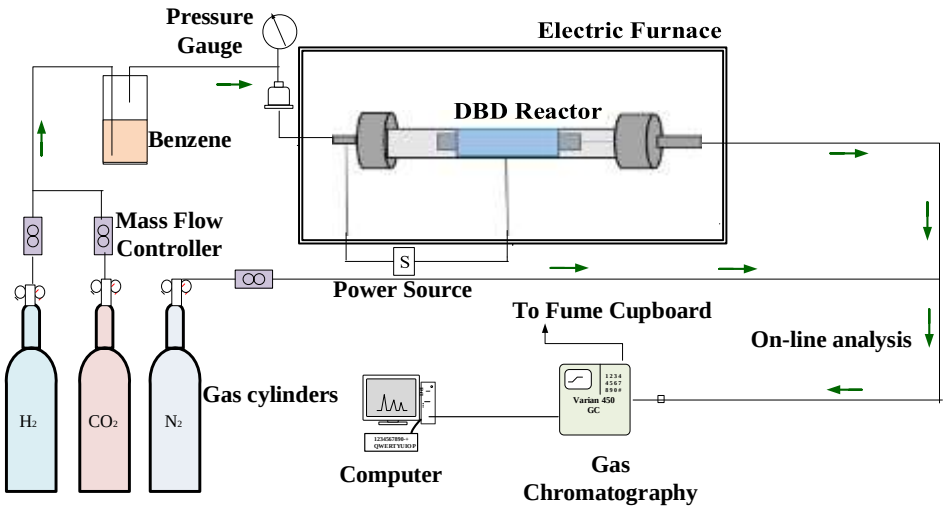

Fig.1. Schematic diagram of the experimental setup

The flow rate of carrier gases (40.6-120 ml/min) was controlled by using computer controlled MFC (mass flow controller) .The carrier gas passes through the benzene (99.8 % anhydrous, sigma-Aldrich) bubbler to saturate with desired amount of benzene. To study the thermal effect on the distribution of the products, an electric furnace was used. The DBD reactor was placed inside a furnace to control the temperature between ambient and 400 ^{o}C.

The product compositions were monitored by a Varian 40-GC equipped with TCD (Thermal conductivity detector) to measure CH_4 and H_2, and FID (Flame ionization detector) to measure the hydrocarbons.

2.2 Definitions of Quantities

Benzene conversion is defined as:

$$d_T = \frac{[C_6H_6]_{in} - [C_6H_6]_{out}}{[C_6H_6]_{in}} \times 100$$

The following formulae were used to calculate the selectivity of different products:

$$\text{LHC selectivity (\%)} = \frac{\sum (\text{m} \times \text{moles of} C_mH_n)}{6 \times \text{Moles of } C_6H_6 \text{ converted}} \times 100$$

$$H_2 \text{ selectivity (\%)} = \frac{\text{moles of } H_2 \text{ produced}}{3 \times \text{ Moles of } C_6H_6 \text{ converted}} \times 100$$

$$\text{CO yield (\%)} = \frac{[\text{moles of CO}]_{out}}{[6 \times C_6H_6 \text{ moles}]_{in} + [CO_2 \text{ moles}]_{in}} \times 100$$

$$\text{Specific input energy } (\frac{\text{kJ}}{\text{L}}) = \frac{\text{P (W)} \times 60/1000}{\text{Flow rate total (L/min)}}$$

The energy efficiency was calculated as follows:

$$\text{Energy efficiency } (\frac{\text{g}}{\text{kWh}}) = \frac{\text{amount of benzene converted (g/min)}}{\text{P (W)} \times 60/3600000}$$

3. Results and discussion

3.1 Effect of carrier gas and SIE

Figure 2 (a) shows the effect of changing the specific input energy (SIE) in CO_2 and H_2. The conversion of benzene was similar for each type of carrier gas at high SIE (above 30 kJ/L). The SIE was increased by increasing the input power (5-40 W). It has been reported that the most of the energy supplied by providing electric fields is absorbed by electrons rather than heavy species (ions, molecules and gas atoms) [32]. At higher powers, the number of high energy

126 electrons increases, so the probability of decomposing benzene (by electron impact) increases.
127 Energy efficiency generally decreases with increasing SIE. Similar behaviour has been
128 reported in previous experimental studies [23].

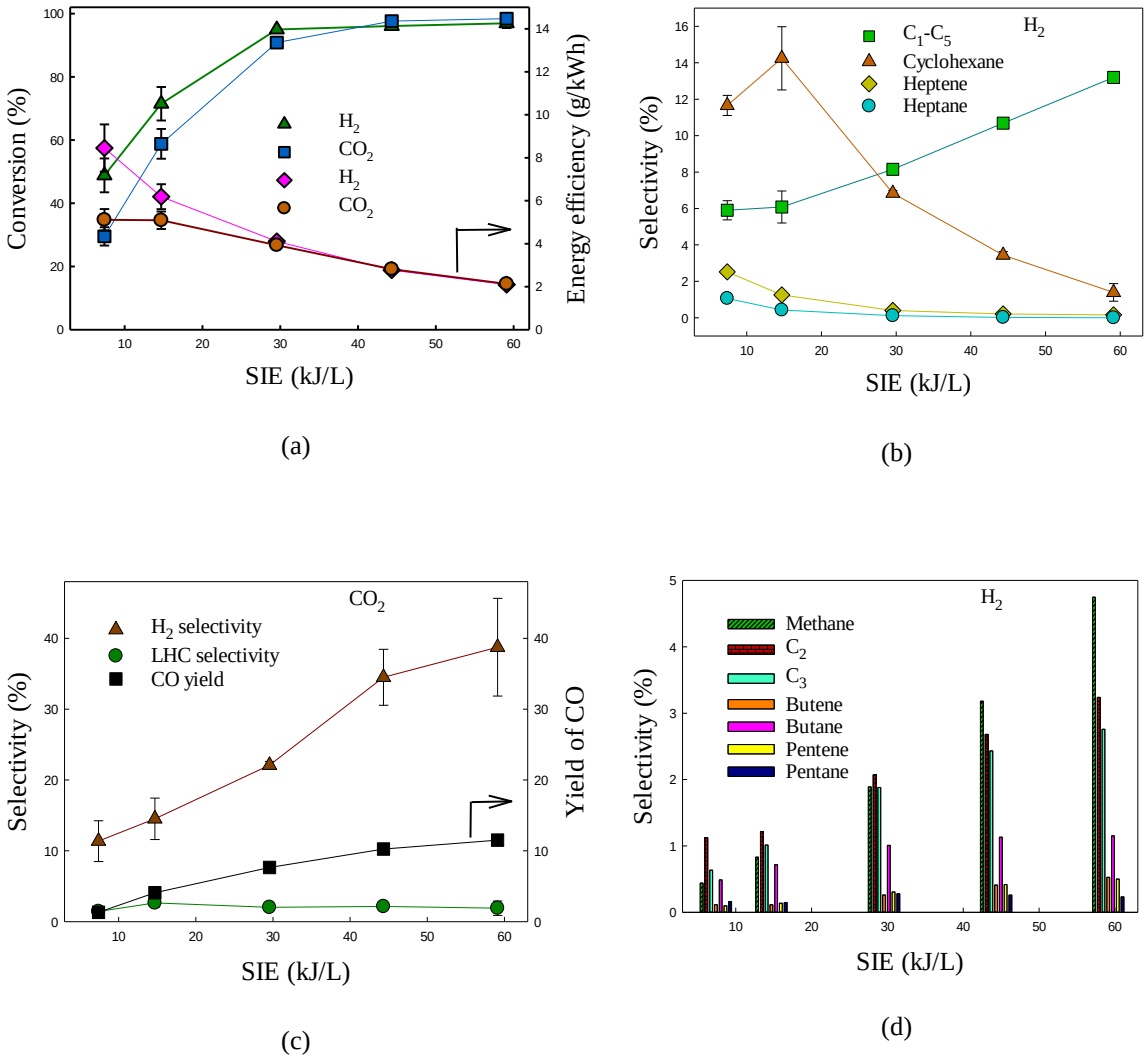

129 **Fig.2** Effect of carrier gas and SIE on: (a) the conversion and energy efficiency of benzene;
130 (b) Selectivity of products in H_2 carrier gas; (c) Selectivity of products in CO_2 carrier gas; and
131 (d) Detailed selectivity to LHC. (Reaction conditions: concentration = 36 g/Nm^3;
132 Temperature=ambient; and residence time=4.23 s)

Below 35 kJ/L, the conversion in the H_2 carrier gas was higher than that for the CO_2. This may be due to production of more reactive H radicals at lower powers, as the bond dissection energy of H_2 (4.53 eV) is lower than that of CO_2 (5.5 eV) [33].

$$e^* + CO_2 \rightarrow O + CO + e \quad (1)$$

$$e^* + H_2 \rightarrow H^{\cdot} + H^{\cdot} + e \quad (2)$$

Fig. 2 (a) also shows the energy efficiency of the process. It can be observed that, below 30 kJ/L, the higher energy efficiency is obtained in H_2 carrier gas. At higher SIE (>35 kJ/L), the energy efficiencies converge. In the absence of plasma, the decomposition of benzene was not observed even at 400 ^oC. It was reported that only 2-3 % conversion of benzene was observed in a sand bed at 650 ^oC. However, the complete conversion occurred at same temperature in the presence of H_2 and Fe_2O_3 catalyst [34]. However, in the absence of catalyst, only 40 % of benzene conversion was observed even above 1200 ^oC, and the reactivity of benzene was minimum as compared to toluene and naphthalene [35]. The non-thermal plasma produces reactive species due to impact of electrons, which have mean energy in the range of 1-10 eV. The reactive atmosphere of active species play a vital role for the decomposition of aromatic compounds

Fig.2 (b) shows the selectivity to hydrocarbons in H_2 carrier gas. It can be seen that the selectivity to LHC (C_1-C_5) increases with specific input energy, but heptane and heptane decrease. The selectivity to cyclohexane increased up to 14.7 kJ/L and then decreased. Equation 2 shows that H radicals (4.5 eV) produced in the plasma discharged due to the impact of energetic electrons [33]. These reactive H radicals are responsible for the hydrogenation reactions of benzene. However, with increasing SIE, due to the increased abundance of electrons, cyclic and long chain compounds began to be converted into lower hydrocarbons.

Hence, it can be observed in Fig. 2 (d) that the selectivity to C_1-C_3 significantly increased with increasing SIE.

In CO_2 carrier gas, the main products were, CO, H_2, LHCs and solid residue. Fig.2 (c) shows the selectivity and yield of gaseous products. The selectivity to lower hydrocarbons remained below 2% at all tested powers due to the presence of O radicals which promote CO and H_2 formation [23]. It can be observed that the selectivity and yield of H_2 and CO also increased with SIE due to increase in the number of reactive species with power.

It was found that formation of solid residue occurred in both carrier gases. The colour of the solid residue was light yellow in hydrogen carrier gas, and black and brown in CO_2. The solid residue formation occurred due to oxygen deficit environment. These solid residues will eventually foul the DBD reactor, and are not desired products. Conversion to these residues must be decreased for plasma processing to present a feasible solution to this problem (tar production). Fig. 3 shows the proposed mechanisms of benzene decomposition under plasma conditions:

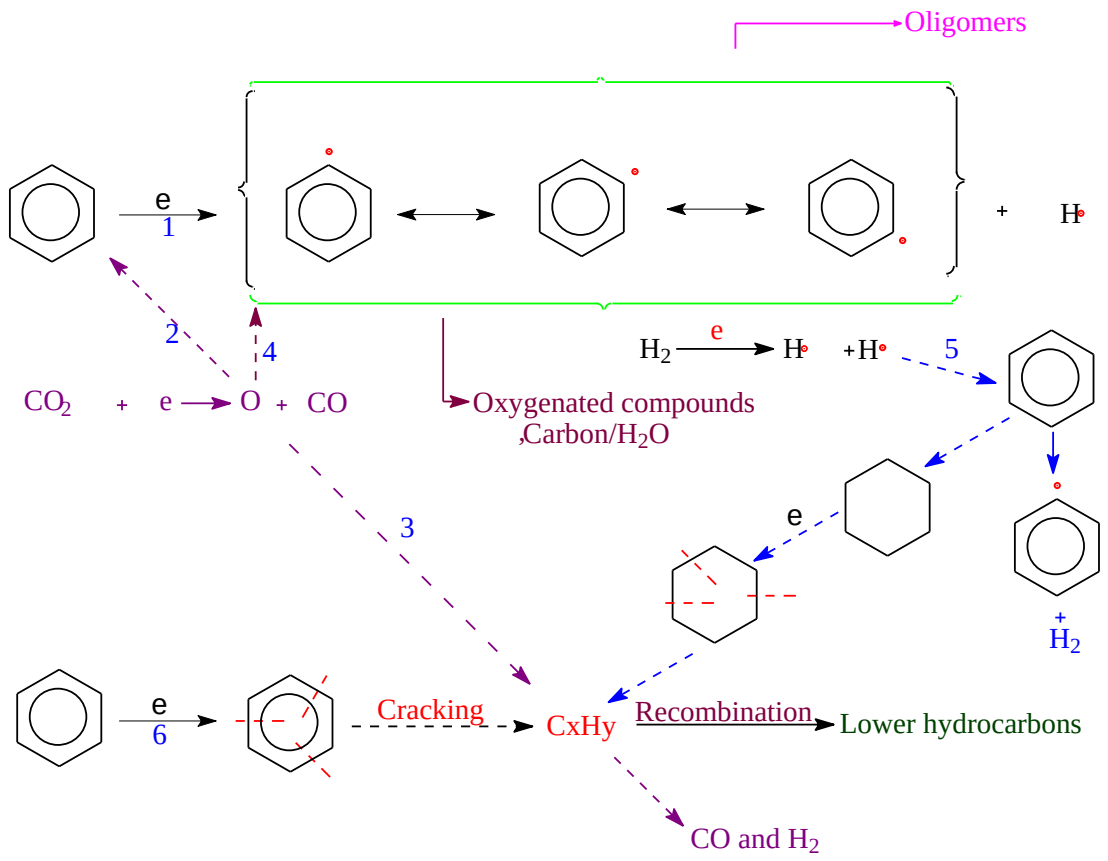

168

169 **Fig.3**. General Mechanism for benzene decomposition

170

171 The first impact of the electron or excited species can abstract the H atom from benzene, as the
172 C-H bond dissociation energy is the minimum in the benzene molecule [33]. Therefore,
173 cracking of benzene could begin through this route and produce the phenyl radicals. These
174 radicals react together to produce solid residue/benzene derivatives. The hydrogenation of
175 benzene through H radicals can also produce cyclohexane. The second impact of high energy
176 electrons may decompose the aromatic ring and cyclic compound to produce straight chain
177 hydrocarbons (path 6). Two mechanisms have been reported for the decomposition of aromatic
178 compounds: direct impact of electrons, and due to collision of gas-phase radicals with aromatic
179 compounds [35]. Reaction mechanism 1 is initiated by collisions between benzene molecules

and energetic electrons in the plasma discharge zone in both carrier gases, resulting in the production of intermediate radicals (phenyl).

Reaction route 2 is initiated by collision of reactive radical (produced due to impact of electrons) and benzene molecules. In fig. 3, route 2 and 5 shows that reactive radicals react with benzene directly to initiate the decomposition process. However, these reactive radicals also can react with intermediates to produce final stable product. Route 3 and 4 shows that O radicals can also react with intermediate to produce oxygenated compounds.

Therefore, in the CO_2 carrier gas, due to presence of nascent oxygen atoms, the intermediate can oxidize to CO and H_2.

3.2 Effect of residence time.

The effect of residence time on the conversion of benzene in both carrier gases is shown in fig.4 (a). The effect of changing the residence time on conversion in each carrier gas is the same: increasing with increasing residence time. At high residence time, the benzene molecules spend more time in discharge zone, which allow them to interact with the reactive species for longer. In this way, higher residence time promotes the conversion of benzene due to the increased number of collision between tar analogue and discharge species [23].

Fig. 4 (a) shows the effect of residence time on the energy efficiency of the plasma process. As Residence time and conversion increase, the energy efficiency decreases. To enhance the energy efficiency of the process, the residence time and power need to be optimized for the desired conversion of benzene.

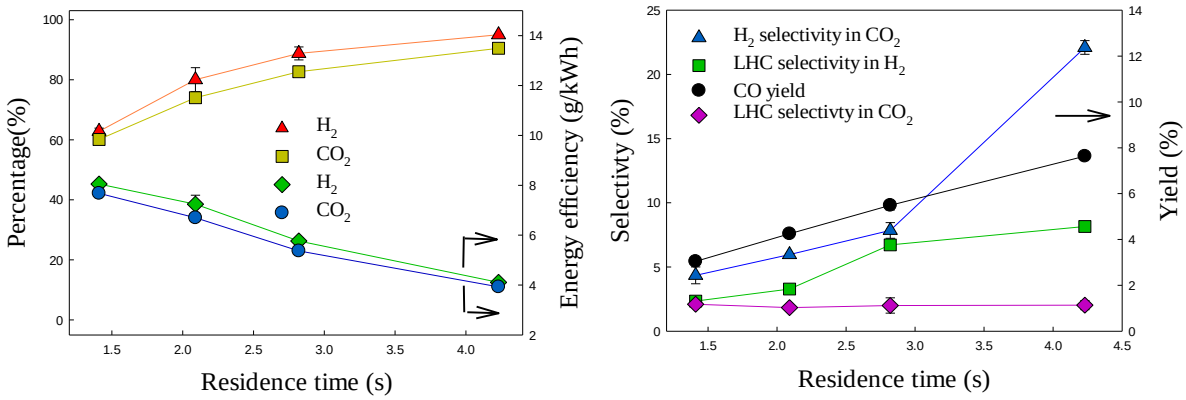

(a) (b)

Fig.4 Effect of residence time on: (a) the conversion and energy efficiency of benzene; (b) selectivity and yield of products, in H_2 and CO_2 (Reaction conditions: concentration = 36 g/Nm^3; Temperature=ambient; and plasma power=20 W)

Fig.4 (b) shows the selectivity of lower hydrocarbons (LHC). It can be noted that hydrogen gives maximum selectivity due to the rich environment of H radicals which combine with the fragments of benzene. The selectivity shows increasing trend with respect to residence time in H_2. The reason may be that the number of collisions between H radicals and aromatic intermediate species increases when increasing residence time. Therefore, the selectivity of lower hydrocarbons increases due to high collision frequency of these species with H radicals.

However in CO_2 the selectivity of lower hydrocarbons does not increase above 2 % due to presence of oxygen which oxidizes the intermediate compounds into CO and H_2

The selectivity and yield of H_2 and CO are shown in Fig. 2(b). It can be observed that both the selectivity and yield of products increase with increasing residence time. The trend is consistent with previous experimental studies in which the decomposition of toluene was studied in a rotating gliding arc discharge reactor [17].

3.3 Effect of Concentration

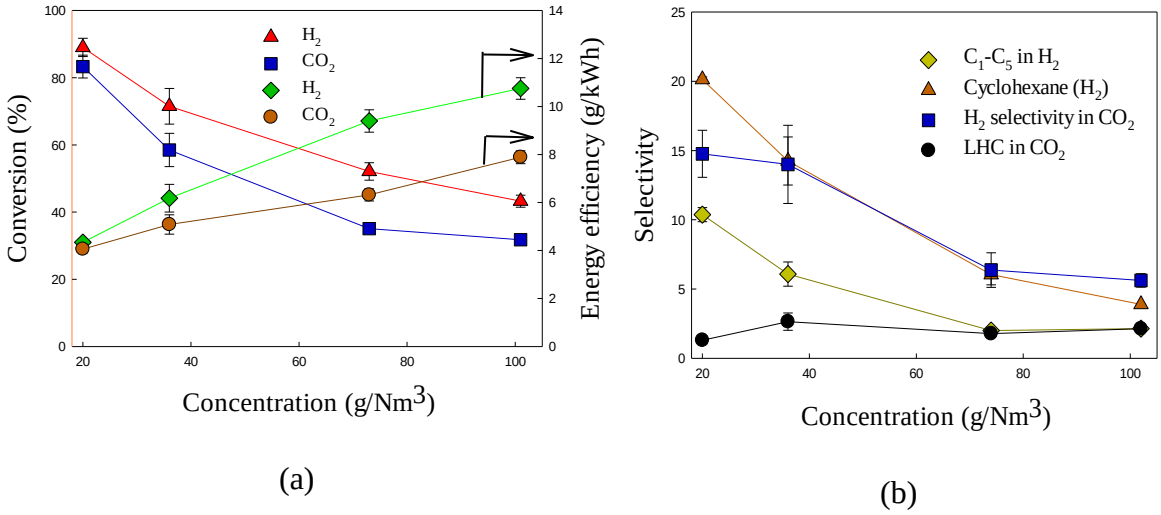

Fig.5 Effect of concentration in each carrier gas on: (a) the conversion and energy efficiency of benzene; (b) Products selectivity (%). (Reaction conditions: SIE= 14.7 (kJ/ L) Temperature=ambient; and power=10 W**)**

Fig. 5 (a) shows the effect of concentration on the conversion and energy efficacy of benzene in CO_2 and H_2 carrier gases. It can be observed from the figure that the removal efficiency of benzene decreases with increasing concentration. This is because the number of molecules in the discharge zone increases with concentration, while all the other parameters (power, residence time, discharge length) remain constant. Therefore, the chances of unconverted benzene molecules escaping the discharge zone increases. Fig.5 (a) shows that the energy efficiency of the process increases in both carrier gases with increasing concentration. This is because when the input concentration of benzene increases, it also raises the total no. of decomposed molecules.

Fig.5 (b) shows the selectivity of different products in each carrier gas. As concentration increases, selectivity to LHCs and cyclohexane decreases. This is probably due to decrease in the relative amount of reactive species with respect to benzene molecules. At higher concentration more molecules were subjected to discharge zone, whereas the concentration of

electrons remains constant. Thereby, the selectivity to lower hydrocarbons decreases when increasing the concentration. These results are consistent with previous experimental studies on toluene [23].

3.4 Effect of temperature

The effect of temperature on the conversion of benzene can be observed in Fig.6 (a). It can be seen that the conversion of benzene is not influenced by temperature up to 300 ^{o}C, whereas after that it decreases with increasing temperature up to 400 ^{o}C in CO_2. This may be due to radical termination reactions of CO and O, which reduce the reactive species in plasma discharge. It has been reported that termination of radicals can occur via reactions 3 [36].

$$O+CO \rightarrow CO_2 \qquad k = 1.7\times 10^{-33} \exp\left(-\frac{1510}{T}\right) \qquad (2)$$

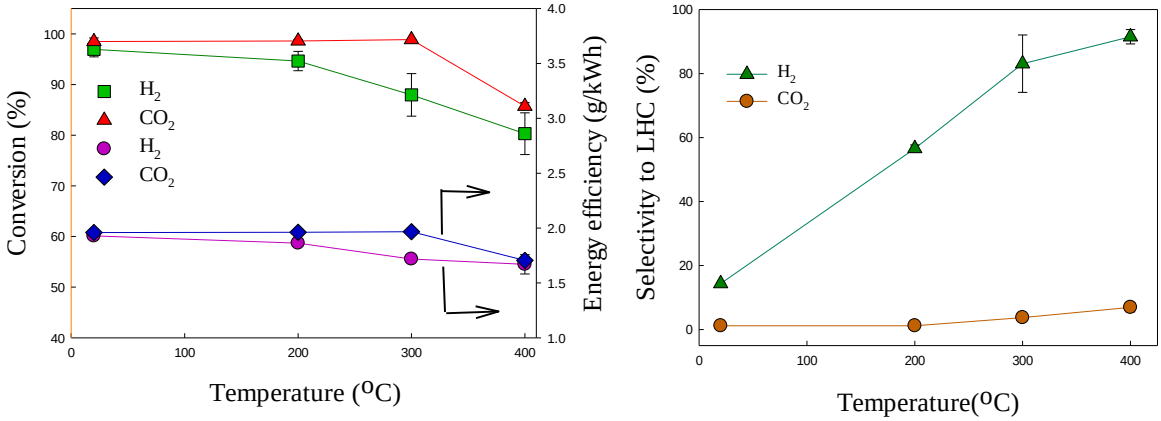

(a) (b)

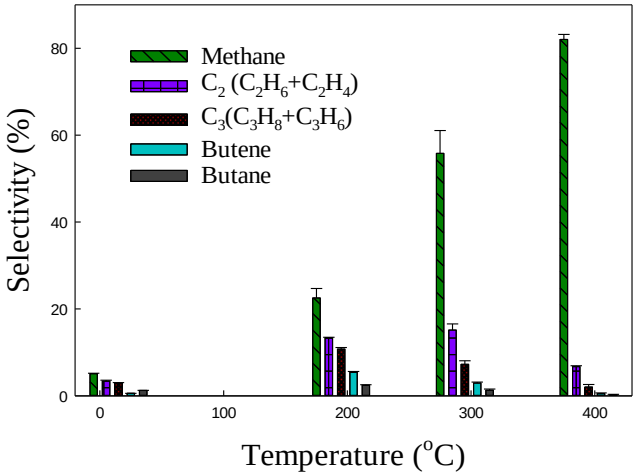

(c)

Fig.6 Effect of temperature and carrier gas on: (a) the conversion and energy efficiency of benzene ; (b) selectivity to lower hydrocarbons; and (d) selectivity to individual LHC in H_2 carrier gas .(Reaction conditions: concentration = 33 g/Nm^3; residence time=4.23 s; power=40 W; and SIE= 59.1 kJ/L)

However, the decomposition of benzene gradually decreases with increasing temperature up to 400 ^oC. A possible route is that plasma produces phenyl radicals by abstracting H from benzene, as the C-H has the minimum bond dissociation energy. These benzyl radicals polymerize and produce solid residue at ambient temperature. However, as the temperature is increased, due to presence of excess reactive H radicals in H_2 carrier gas, it may react with H radicals and reproduce the benzene [37].

Clearly, (fig. 6 a) the decomposition of benzene decreases with increasing temperatures. However, it previously been noted that the conversion of toluene did not change when increasing the temperature at 40 W. Fig. 6 (a) also shows that the energy efficiency of the process decreases due to the decrease in the conversion of benzene, which ultimately reduces amount of decomposed toluene.

Fig. 6 (b) shows the selectivity to LHC (C_1-C_5) with respect to temperature. It can be observed that the selectivity in CO_2 carrier gas slightly increases with increasing the temperature, but in H_2 carrier gas, it increases significantly from 13 % to 91 % with increasing the temperature from ambient to 400 ^oC. Hence, it is clear that the H_2 carrier gas promotes the ring opening reactions and promotes the formation of lower hydrocarbons and eliminates the solid residue formation. This is possible because the plasma discharge produces reactive H radicals which crack benzene fragments and intermediates to lower hydrocarbons at elevated temperatures. In a previous study, the synergetic effect of plasma and temperature was studied on the hydrocracking of toluene using a dielectric barrier discharge reactor [38]. It was observed that nearly complete conversion of toluene to lower hydrocarbons (C_1-C_6) occurred at elevated temperatures under plasma conditions. However, significant amounts of benzene (28%) were observed at elevated temperatures along with methane (60%) depending upon power. It was reported that hydrogen radicals promote the ring opening products at elevated temperatures in the presence of plasma [39]

Fig.6 (c) shows the detailed selectivity to lower hydrocarbons. It can be seen that the selectivity to methane increases from 5.2 to 82 % with increasing the temperature. For C_2, selectivity increases up to 300 ^oC and after which it decreases, while for C_3-C_5, selectivity started to decrease even after 200 ^oC. Therefore, increasing the temperature under plasma conditions promotes the formation of methane from benzene at elevated temperature instead the production of $>C_2$.

It has been reported that thermal decomposition of aromatic compounds requires temperatures in the range 500-1200 ^oC [40, 41]. It has been observed that the yield of methane doubles (11.7 to 23.8 wt. %) with increasing the temperature from 800 to 850 ^oC, whereas the yield of C_2H_4 and C_3H_8 decreases [42] . Therefore, it could be suggested that increasing temperature favours

281 the conversion of C_2H_4 and C_3H_8 to CH_4. However, in this study, these reactions took place at
282 lower temperature ranges (20-400 ^oC).

283 It was noted that the input energy played a key role in the decomposition of the benzene. The
284 rate equation for the cracking of benzene with respect to SIE can be written as

285

$$r = -d[C_6H_6]/\,dSIE = k_{SIE}[C_6H_6]^n \quad (6)$$

286 Here k_{SIE} is an energy constant and n is a reaction order. Fig. 7 a plot of ln (C/C_o) exhibits a
287 straight line in both carrier gases. Therefore, the benzene removal in both carrier gases can be
288 written as

$$ln\frac{[C_6H_6]}{[C_6H_6]_0} = -k_{SIE} \times SIE \quad (7)$$

289

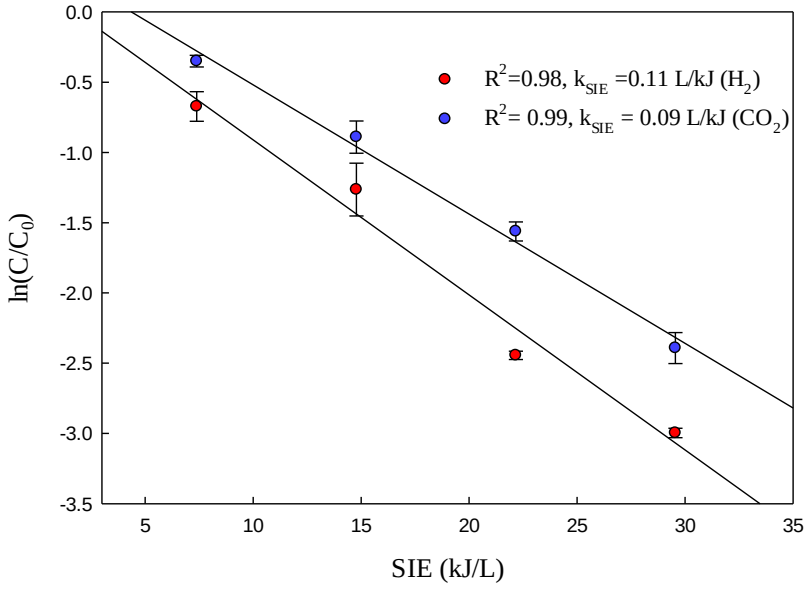

290

291 **Fig.7** Effect of specific input energy (SIE) on the remaining fraction of benzene
292 (Reaction conditions: concentration = 36 g/Nm^3; Temperature=ambient; and
293 residence time=4.23 s)

294

295 In CO_2 and H_2, the value of R^2 are 0.98 and 0.99 respectively. Hence, the decomposition of
296 benzene in DBD reactor with respect to SIE shows first order kinetics.

297

298 **4. Conclusions**

299 In this study, a DBD reactor was used to investigate the conversion of benzene, acting as a tar
300 analogue, in CO_2 and H_2 carrier gases. The parameters studied were SIE (7-59 kJ/L), residence
301 time (1.41-4.23 s), concentration (20-102 g/Nm^3) and temperature (ambient-400 ^oC).

302 The main findings were:

303 1. At high SIEs, the conversion of benzene was similar in both carrier gases, due to the
304 high population of reactive species. However, at lower SIEs (<30 kJ/L), there was a
305 clear difference, and the H_2 exhibited significantly higher conversions of benzene than
306 the CO_2. This is due to the higher reactivity of the H free radical.
307 2. The decomposition of benzene increased with increasing SIE and residence time in
308 either carrier gas, and decreased with increasing concentration. The quantification of
309 these effects should allow NTP DBD reactor design
310 3. The wall temperature of the reactor was identified as an important parameter in
311 controlling the product distribution. Importantly, it was noted that solid formation
312 completely disappeared in H_2 carrier gas at 400 ^oC, and the selectivity to LHC was as
313 high as 91 %. The presence of H radicals at elevated temperatures in the presence of
314 plasma promoted the new reaction route to crack the aromatic ring and intermediates to
315 lower hydrocarbons .Therefore these reactors can be operated without solid residue
316 formation in the presence of H_2 carrier gas at elevated temperatures along with NTP.

4. At higher powers and temperatures (40 W and 400 ^{o}C) selectivity to methane increased from 5.2 to 82 % in H_2 carrier gas, whereas, the selectivity to C_2-C_4 decreased from 28 % to 8 % with increasing temperature from 300 to 400 ^{o}C at 40 W. Clearly, hydrocarbon chain length can be controlled by judicious choice of wall temperature: chain length decreases as temperature increases.

These results illustrate the opportunities for combining thermal effects with non-thermal plasma effects for operation of gas phase reactors. In this case, judicious choice of temperature could be used to operate the reactor such that no solid residue was formed, and the "tar" was largely converted into methane.

References

[1] H. Hofbauer, G. Veronik, T. Fleck, R. Rauch, H. Mackinger, E. Fercher, The FICFB—gasification process, Developments in thermochemical biomass conversion, Springer1997, pp. 1016-1025.

[2] K. Sato, K. Fujimoto, Development of new nickel based catalyst for tar reforming with superior resistance to sulfur poisoning and coking in biomass gasification, Catalysis Communications 8 (2007) 1697-1701.

[3] E. Gusta, A.K. Dalai, M.A. Uddin, E. Sasaoka, Catalytic decomposition of biomass tars with dolomites, Energy & Fuels 23 (2009) 2264-2272.

[4] Y. Richardson, J. Blin, A. Julbe, A short overview on purification and conditioning of syngas produced by biomass gasification: catalytic strategies, process intensification and new concepts, Progress in Energy and Combustion Science 38 (2012) 765-781.

340 [5] S. Anis, Z.A. Zainal, Tar reduction in biomass producer gas via mechanical, catalytic and thermal
341 methods: A review, Renewable and Sustainable Energy Reviews 15 (2011) 2355-2377.
342 [6] P. Basu, Biomass Gasification and Pyrolysis: Practical Design and Theory, Elsevier Science2010.
343 [7] Y. Chen, Y.-h. Luo, W.-g. Wu, Y. Su, Experimental investigation on tar formation and destruction in
344 a lab-scale two-stage reactor, Energy & Fuels 23 (2009) 4659-4667.
345 [8] G.-Y. Chen, C. Liu, W.-C. Ma, B.-B. Yan, N. Ji, Catalytic Cracking of Tar from Biomass Gasification
346 over a HZSM-5-Supported Ni–MgO Catalyst, Energy & Fuels 29 (2015) 7969-7974.
347 [9] A.W. Bosmans, S; Helsen, L, Waste to clean syngas: Avoiding Tar Problems, 2nd International
348 Enhanced Landfill Mining Symposium (2013).
349 [10] A. Bosmans, S. Wasan, L. Helsen, Waste-to-clean syngas: avoiding tar problems, Proceedings of
350 the 2nd International Academic Symposium on Enhanced Landfill Mining, Haletra, 2013, pp. 181-201.
351 [11] W. Wang, N. Padban, Z. Ye, G. Olofsson, A. Andersson, I. Bjerle, Catalytic hot gas cleaning of fuel
352 gas from an air-blown pressurized fluidized-bed gasifier, Industrial & engineering chemistry research
353 39 (2000) 4075-4081.
354 [12] D.N. Bangala, N. Abatzoglou, J.-P. Martin, E. Chornet, Catalytic gas conditioning: application to
355 biomass and waste gasification, Industrial & Engineering Chemistry Research 36 (1997) 4184-4192.
356 [13] M.A. Caballero, J. Corella, M.-P. Aznar, J. Gil, Biomass gasification with air in fluidized bed. Hot gas
357 cleanup with selected commercial and full-size nickel-based catalysts, Industrial & Engineering
358 Chemistry Research 39 (2000) 1143-1154.
359 [14] M.P. Aznar, M.A. Caballero, J. Gil, J.A. Martin, J. Corella, Commercial steam reforming catalysts to
360 improve biomass gasification with steam− oxygen mixtures. 2. Catalytic tar removal, Industrial &
361 Engineering Chemistry Research 37 (1998) 2668-2680.
362 [15] A.J.M. Pemen, S.A. Nair, K. Yan, E.J.M. Van Heesch, K.J. Ptasinski, A.A.H. Drinkenburg, Pulsed
363 corona discharges for tar removal from biomass derived fuel gas, Plasmas and polymers 8 (2003) 209-
364 224.

365 [16] P. Jamróz, W. Kordylewski, M. Wnukowski, Microwave plasma application in decomposition and
366 steam reforming of model tar compounds, Fuel Processing Technology 169 (2018) 1-14.
367 [17] F. Zhu, X. Li, H. Zhang, A. Wu, J. Yan, M. Ni, H. Zhang, A. Buekens, Destruction of toluene by
368 rotating gliding arc discharge, Fuel 176 (2016) 78-85.
369 [18] S. Liu, D. Mei, L. Wang, X. Tu, Steam reforming of toluene as biomass tar model compound in a
370 gliding arc discharge reactor, Chemical Engineering Journal 307 (2017) 793-802.
371 [19] O. Karatum, M.A. Deshusses, A comparative study of dilute VOCs treatment in a non-thermal
372 plasma reactor, Chemical Engineering Journal 294 (2016) 308-315.
373 [20] N. Blin-Simiand, F. Jorand, L. Magne, S. Pasquiers, C. Postel, J.R. Vacher, Plasma reactivity and
374 plasma-surface interactions during treatment of toluene by a dielectric barrier discharge, Plasma
375 Chemistry and Plasma Processing 28 (2008) 429-466.
376 [21] B. Wang, C. Chi, M. Xu, C. Wang, D. Meng, Plasma-catalytic removal of toluene over CeO2-MnOx
377 catalysts in an atmosphere dielectric barrier discharge, Chemical Engineering Journal 322 (2017) 679-
378 692.
379 [22] H.M. Lee, M.B. Chang, Abatement of gas-phase p-xylene via dielectric barrier discharges, Plasma
380 chemistry and plasma processing 23 (2003) 541-558.
381 [23] F. Saleem, K. Zhang, A. Harvey, Role of CO2 in the Conversion of Toluene as a Tar Surrogate in a
382 Nonthermal Plasma Dielectric Barrier Discharge Reactor, Energy & Fuels (2018).
383 [24] H.J. Park, S.H. Park, J.M. Sohn, J. Park, J.-K. Jeon, S.-S. Kim, Y.-K. Park, Steam reforming of biomass
384 gasification tar using benzene as a model compound over various Ni supported metal oxide catalysts,
385 Bioresource Technology 101 (2010) S101-S103.
386 [25] Y.N. Chun, S.C. Kim, K. Yoshikawa, Decomposition of benzene as a surrogate tar in a gliding Arc
387 plasma, Environmental Progress & Sustainable Energy 32 (2013) 837-845.
388 [26] Y.N. Chun, S.C. Kim, K. Yoshikawa, Removal characteristics of tar benzene using the externally
389 oscillated plasma reformer, Chemical Engineering and Processing: Process Intensification 57 (2012)
390 65-74.

391 [27] Y.N. Chun, M.S. Lim, Light tar decomposition of product pyrolysis gas from sewage sludge in a
392 gliding arc plasma reformer, Environmental Engineering Research 17 (2012) 89-94.
393 [28] P.A. Simell, N.A.K. Hakala, H.E. Haario, A.O.I. Krause, Catalytic decomposition of gasification gas
394 tar with benzene as the model compound, Industrial & engineering chemistry research 36 (1997) 42-
395 51.
396 [29] P.A. Simell, E.K. Hirvensalo, V.T. Smolander, A.O.I. Krause, Steam reforming of gasification gas tar
397 over dolomite with benzene as a model compound, Industrial & Engineering Chemistry Research 38
398 (1999) 1250-1257.
399 [30] R. Zhang, Y. Wang, R.C. Brown, Steam reforming of tar compounds over Ni/olivine catalysts doped
400 with CeO2, Energy Conversion and Management 48 (2007) 68-77.
401 [31] M. He, Z. Hu, B. Xiao, J. Li, X. Guo, S. Luo, F. Yang, Y. Feng, G. Yang, S. Liu, Hydrogen-rich gas from
402 catalytic steam gasification of municipal solid waste (MSW): influence of catalyst and temperature on
403 yield and product composition, International Journal of Hydrogen Energy 34 (2009) 195-203.
404 [32] U.R. Kortshagen, R.M. Sankaran, R.N. Pereira, S.L. Girshick, J.J. Wu, E.S. Aydil, Nonthermal plasma
405 synthesis of nanocrystals: fundamental principles, materials, and applications, Chemical reviews 116
406 (2016) 11061-11127.
407 [33] B.d. Darwent, Bond dissociation energies in simple molecules, NSRDS-NBS NO. 31, U. S. DEPT.
408 COMMERCE, WASHINGTON, D. C. JAN. 1970, 48 P (1970).
409 [34] S.S. Tamhankar, K. Tsuchiya, J.B. Riggs, Catalytic cracking of benzene on iron oxide-silica: catalyst
410 activity and reaction mechanism, Applied Catalysis 16 (1985) 103-121.
411 [35] W.-J. Liang, L. Ma, H. Liu, J. Li, Toluene degradation by non-thermal plasma combined with a
412 ferroelectric catalyst, Chemosphere 92 (2013) 1390-1395.
413 [36] A. Cenian, A. Chernukho, V. Borodin, Modeling of Plasma-Chemical Reactions in Gas Mixture of
414 CO2 lasers. II. Theoretical Model and its Verification, Contributions to Plasma Physics 35 (1995) 273-
415 296.

[37] L.B. Harding, Y. Georgievskii, S.J. Klippenstein, Predictive theory for hydrogen atom− hydrocarbon radical association kinetics, The Journal of Physical Chemistry A 109 (2005) 4646-4656.

[38] F. Saleem, K. Zhang, A. Harvey, Temperature dependence of non-thermal plasma assisted hydrocracking of toluene to lower hydrocarbons in a dielectric barrier discharge reactor, Chemical Engineering Journal 356 (2019) 1062-1069.

[39] F. Saleem, K. Zhang, A. Harvey, Plasma-assisted decomposition of a biomass gasification tar analogue into lower hydrocarbons in a synthetic product gas using a dielectric barrier discharge reactor, Fuel 235 (2019) 1412-1419.

[40] A. Jess, Mechanisms and kinetics of thermal reactions of aromatic hydrocarbons from pyrolysis of solid fuels, Fuel 75 (1996) 1441-1448.

[41] L. Fagbemi, L. Khezami, R. Capart, Pyrolysis products from different biomasses: application to the thermal cracking of tar, Applied energy 69 (2001) 293-306.

[42] C. Gai, Y. Dong, P. Fan, Z. Zhang, J. Liang, P. Xu, Kinetic study on thermal decomposition of toluene in a micro fluidized bed reactor, Energy Conversion and Management 106 (2015) 721-727.